

Article

Accurate compound-specific ^{14}C dating of archaeological pottery vessels

<https://doi.org/10.1038/s41586-020-2178-z>

Received: 24 May 2019

Accepted: 13 February 2020

Published online: 08 April 2020

 Check for updates

Emmanuelle Casanova¹, Timothy D. J. Knowles^{1,2}, Alex Bayliss^{3,4}, Julie Dunne¹, Marek Z. Barański⁵, Anthony Denaire⁶, Philippe Lefranc⁷, Savino di Lernia^{8,9}, Mélanie Roffet-Salque¹, Jessica Smyth^{1,10}, Alistair Barclay¹¹, Toby Gillard¹, Erich Claßen¹², Bryony Coles¹³, Michael Ilett¹⁴, Christian Jeunesse¹⁵, Marta Krueger¹⁶, Arkadiusz Marciniak¹⁶, Steve Minnitt¹⁷, Rocco Rotunno⁸, Pieter van de Velde¹⁸, Ivo van Wijk¹⁹, Jonathan Cotton²⁰, Andy Daykin²⁰ & Richard P. Evershed^{1,2}✉

Pottery is one of the most commonly recovered artefacts from archaeological sites. Despite more than a century of relative dating based on typology and seriation¹, accurate dating of pottery using the radiocarbon dating method has proven extremely challenging owing to the limited survival of organic temper and unreliability of visible residues^{2–4}. Here we report a method to directly date archaeological pottery based on accelerator mass spectrometry analysis of ^{14}C in absorbed food residues using palmitic ($\text{C}_{16:0}$) and stearic ($\text{C}_{18:0}$) fatty acids purified by preparative gas chromatography^{5–8}. We present accurate compound-specific radiocarbon determinations of lipids extracted from pottery vessels, which were rigorously evaluated by comparison with dendrochronological dates^{9,10} and inclusion in site and regional chronologies that contained previously determined radiocarbon dates on other materials^{11–15}. Notably, the compound-specific dates from each of the $\text{C}_{16:0}$ and $\text{C}_{18:0}$ fatty acids in pottery vessels provide an internal quality control of the results⁶ and are entirely compatible with dates for other commonly dated materials. Accurate radiocarbon dating of pottery vessels can reveal: (1) the period of use of pottery; (2) the antiquity of organic residues, including when specific foodstuffs were exploited; (3) the chronology of sites in the absence of traditionally datable materials; and (4) direct verification of pottery typochronologies. Here we used the method to date the exploitation of dairy and carcass products in Neolithic vessels from Britain, Anatolia, central and western Europe, and Saharan Africa.

Chronology lies at the heart of archaeology¹⁶. Radiocarbon dating by accelerator mass spectrometry (AMS) is the most widely used method for providing calendrical chronologies for human activities over the past 50,000 years¹⁷, and is most commonly performed on samples of charred plant remains and bone¹⁷. Radiocarbon dates can be used alongside relative sequences, such as those derived from stratigraphy or the typological analysis or seriation of artefact types, to build chronological models. Applying Bayes' theorem enables radiocarbon dating to provide calendar age estimates with uncertainties as low as a few decades¹⁸.

The invention of pottery in the late Pleistocene epoch was probably a critical driver for developments in food processing^{19,20}. Pottery vessels can often be placed in robust relative chronological sequences using typology and seriation, although obtaining precise and accurate

radiocarbon dates from pottery is challenging^{2,3,21}. All sources of carbon associated with pottery vessels have been considered for dating^{2–4}, including organic temper, which occasionally survives firing, and superficial food crusts, although these are rare and prone to contamination owing to their exposed nature²². By contrast, the lipidic components of food residues absorbed into—and protected by—the clay matrix during cooking occur very commonly⁸, often in high concentrations (milligrams per gram of clay fabric). These offer an untapped resource for radiocarbon dating. The most common absorbed residues correspond to degraded animal fats characterized by their high abundances of $\text{C}_{16:0}$ and $\text{C}_{18:0}$ fatty acids^{7,8}. The possibility of using preparative capillary gas chromatography (pcGC) to isolate chemically pure fatty acids from such residues for compound-specific radiocarbon analysis (CSRA) was recognized more than 20 years ago^{21,23,24}. Although initial attempts

¹Organic Geochemistry Unit, School of Chemistry, University of Bristol, Bristol, UK. ²Bristol Radiocarbon Accelerator Mass Spectrometry Facility, University of Bristol, Bristol, UK. ³Scientific Dating, Historic England, London, UK. ⁴Biological & Environmental Sciences, University of Stirling, Stirling, UK. ⁵Faculty of Architecture and Design, Academy of Fine Arts in Gdańsk, Gdańsk, Poland. ⁶University of Burgundy/UMR 6298 ARTEHIS, Dijon, France. ⁷University of Strasbourg UMR 7044/INRAP, Strasbourg, France. ⁸Dipartimento di Scienze dell'Antichità, Sapienza, Università di Roma, Rome, Italy. ⁹GAES, University of the Witwatersrand, Johannesburg, South Africa. ¹⁰School of Archaeology, University College Dublin, Dublin, Ireland. ¹¹Cotswold Archaeology, Cirencester, UK. ¹²LVR-State Service for Archaeological Heritage, Bonn, Germany. ¹³Department of Archaeology, University of Exeter, Exeter, UK. ¹⁴Université Paris 1 Panthéon-Sorbonne, UMR 8215 Trajectoires, Nanterre, France. ¹⁵University of Strasbourg, UMR7044, MISHA, Strasbourg, France. ¹⁶Institute of Archaeology, Adam Mickiewicz University, Poznań, Poland. ¹⁷Somerset County Museum, Taunton Castle, Taunton, UK. ¹⁸Archaeological Research Leiden, Leiden, The Netherlands. ¹⁹Faculty of Archaeology, Leiden University, Leiden, The Netherlands. ²⁰Museum of London Archaeology (MOLA), London, UK. ✉e-mail: r.p.evershed@bristol.ac.uk

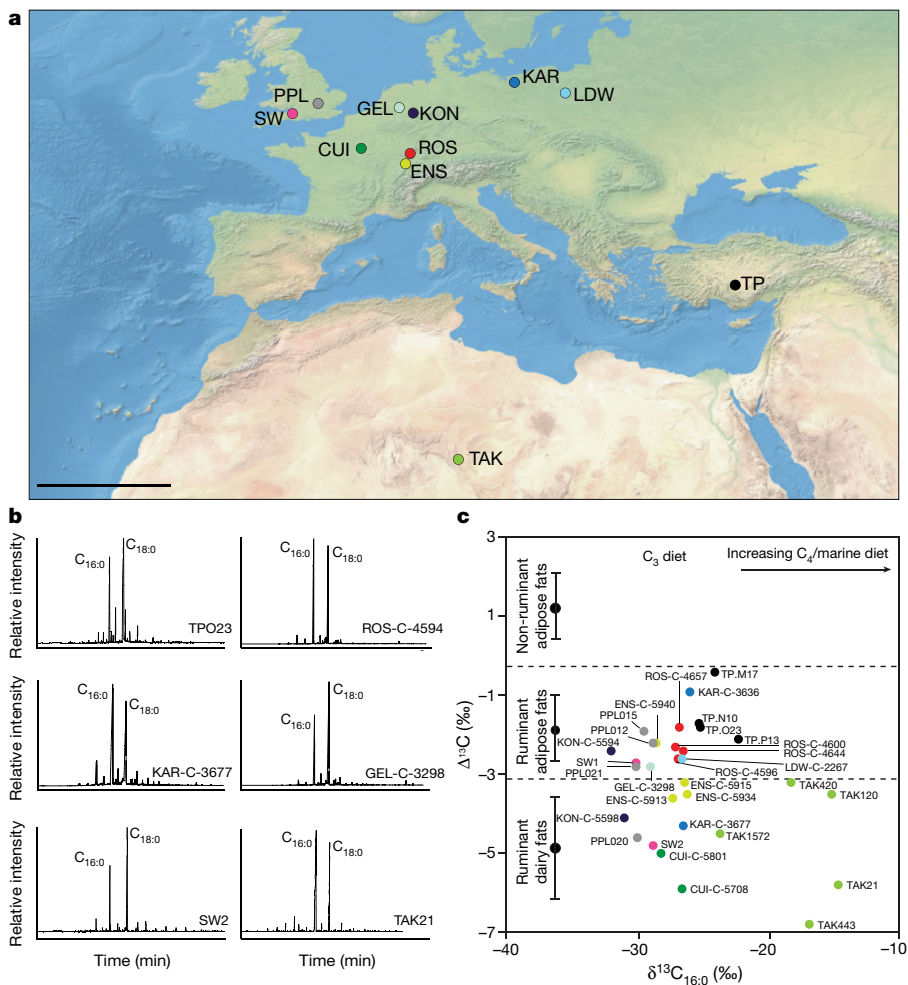


Fig. 1 | Site location map, partial gas chromatograms and stable isotope determination of compound-specific radiocarbon-dated lipid residues preserved in Neolithic pottery vessels. **a**, Map of the location of the archaeological sites for which CSRA was used in this study. Scale bar, 1,000 km. CUI, Cuiry-lès-Chaudardes; ENS, Ensisheim; GEL, Geleen-Janskamperveld; KAR, Karwowo 1; KON, Königshoven 14; LDW, Ludwinowo 7; PPL, Principal

Place, London; ROS, Rosheim; SW, Sweet Track; TAK, Takarkori; TP, Çatalhöyük East. **b**, Partial gas chromatograms of a selection of potsherds showing C_{16:0} and C_{18:0} fatty acid abundances. **c**, Scatter plots of Δ¹³C ($= \delta^{13}\text{C}_{18:0} - \delta^{13}\text{C}_{16:0}$) values plotted against δ¹³C_{16:0} values (mean of 2 measurements) for all of the sherds dated ($n = 31$), ranges on the left denote the mean ± 1 s.d. of modern reference fats, as reported in ref.²⁸.

to date pottery vessels were promising, the accuracy and precision demanded by archaeology could not be achieved owing to unidentified technical difficulties, leading to highly variable results^{21,23}.

We have brought together the latest technologies for radiocarbon measurements, including automated graphitization and MICADAS compact AMS, in conjunction with high-field 700-MHz NMR, to undertake systematic investigations of the pcGC protocol^{5,6}. Rigorous assessment of contamination in compounds purified by pcGC was undertaken, leading to our invention of a solventless pcGC trap and implementation of cleaning procedures to avoid between-run carryover^{5,6}. These advances reduce the exogenous contamination of fatty acids that has previously been associated with pcGC to below concentrations that would significantly affect measured radiocarbon ages. For archaeological animal fats, it has previously been demonstrated that two fatty acids isolated from the same matrix generate the same radiocarbon age (that is, statistically consistent at the 95% significance level), providing an internal quality control for archaeological dating⁶. In this study, we aim to extend this method to archaeological pot lipids. We selected pottery vessels that were rich in animal fats from our database of lipid residues that we accumulated over the last three decades. Pottery vessels from chronologically well-characterized settings and different burial environments were analysed and the compatibility of pot lipid dates with

these existing chronologies was evaluated by statistical comparison of posterior density estimates for the key parameters and the use of indices of agreement with inclusion in these known frameworks (Fig. 1, Extended Data Table 1 and Supplementary Information 1).

We initially focused on Neolithic Carinated Bowl pottery from the Sweet Track (Fig. 2a), an elevated wooden trackway discovered in a wetland area of the Somerset Levels^{9,10,25} in the United Kingdom (Supplementary Information 2). This site is critical because its construction has been precisely dated by dendrochronology to the winter–early spring of 3807–3806 BC and the trackway was used and maintained for approximately 10 years¹⁰. Lipids from pots that were found alongside the trackway, and were probably contemporaneous to its construction and use, have previously been dated, but the measured dates were a century later than the construction of the trackway²³. Re-analysis of the two vessels (Fig. 2b) using our new approach produced uncalibrated radiocarbon ages of $5,110 \pm 25$ years before present (BP; taken as AD 1950) (SW1) and $5,092 \pm 26$ BP (SW2), which are statistically indistinguishable ($T' = 9.0$, $T'(5\%) = 9.5$, $v = 4$) from the measurements of the tree rings included in the IntCal13 calibration curve for the relevant decade²⁶ (Fig. 2c). The calibrated dates of these ages are clearly compatible with the tree-ring dates for the construction of the trackway.

Extending our approach to Anatolia, the Neolithic tell of Çatalhöyük East was a locus for the emergence and development of pottery

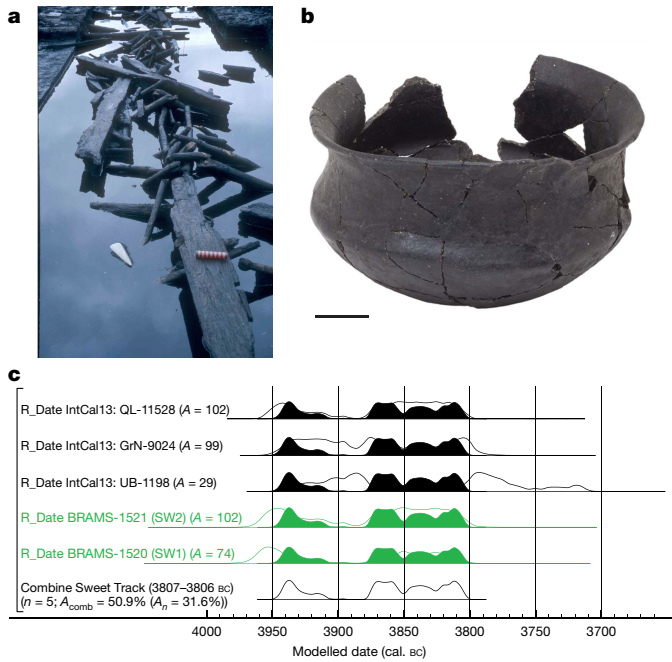


Fig. 2 | Sweet Track timbers, a pottery vessel and calibrated radiocarbon dates. **a**, Photograph of Sweet Track timbers. **b**, Photograph of a Carinated Bowl (SW2) that was recovered alongside the Sweet Track. Scale bar, 5 cm. **c**, Probability distributions of dates from pots deposited next to the Sweet Track (green) and from oak trees (black) included in IntCal13²⁶ that include the date of the Sweet Track construction in 3807–3806 BC. Each distribution represents the relative probability that an event occurs at a particular time. For each of the dates, two distributions have been plotted: one in outline, which is the simple radiocarbon calibration, and a solid distribution, based on the model used. The square bracket down the left side along with the OxCal keywords define the overall model exactly (provided in Supplementary Information 2). A , A_{comb} and A_n are the individual agreement indices, the combination agreement indices and the acceptable threshold to combine n radiocarbon dates, respectively. The photographs were provided by S.M. and are reproduced with permission from the Somerset Levels Project.

production. A 21-m-deep stratigraphic sequence provides strong archaeological prior information for a Bayesian chronological model that covers the upper parts of the mound (TP area)¹¹. The sequence of houses, middens and burial structures has been combined with 50 radiocarbon dates, revealing a Neolithic sequence of occupation from the mid-sixty-fourth to the mid-sixtieth centuries calibrated (cal.) BC¹¹. Our compound-specific radiocarbon ages on adipose lipids²⁷ from four pottery vessels from four different contexts (TP.M17, $7,382 \pm 31$ BP; TP.N10, $7,348 \pm 25$ BP; TP.O23, $7,340 \pm 27$ BP; and TP.P13, $7,364 \pm 25$ BP) were incorporated into the Bayesian chronological model for this part of the site (Extended Data Figs. 1, 2 and Supplementary Information 3). The revised model for the Neolithic deposits in the TP area shows posterior distributions for the key parameters that are almost identical to those from the original model¹¹. Their median values vary by an average of 4 years and a maximum of 10 years, confirming the compatibility of the radiocarbon ages determined using fatty acids with the site stratigraphy. On the basis of sensitivity analyses (Supplementary Information 3), this well-constrained model is at least as sensitive as measurements on paired materials to detect inaccuracies. In this case, the CSRA dates not only provide direct dating for the importance of ruminant carcass products (Fig. 1c) to the inhabitants of Çatalhöyük at this time (derived from $\delta^{13}\text{C}$ values of preserved fats), but also provide direct dating evidence for the climatic changes associated with the global event of 8.2 thousand years ago (derived from compound-specific deuterium isotope analyses using the same fats)²⁷.

The next analysis tests the accuracy of our dating approach using a classic pottery seriation study related to Neolithic ceramics from Lower Alsace (France) that spans the second quarter of the fifth millennium cal. BC¹² (Supplementary Information 4). The regional correspondence analysis clearly separates the Hinkelstein, Grossgartach, Planig-Friedberg and Rössen Middle Neolithic ceramic groups. We focused on vessels from three pits, all of which can be assigned to the Grossgartach phase (Fig. 3a, b). The sequence of ceramic phases was combined with the existing assemblage of 95 radiocarbon dates, which were largely measured on articulated bones, along with four CSRA dates on fatty acids (ROS-C-4596, $5,804 \pm 25$ BP; ROS-C-4600, $5,904 \pm 28$ BP; ROS-C-4644, $5,931 \pm 26$ BP; and ROS-C-4657, $5,912 \pm 28$ BP) from the Grossgartach sherds in a model using Bayesian statistics. The phase boundaries in this revised model are very similar to those produced by the original analysis¹², as median values differ by an average of 6 years and a maximum of 15 years (Fig. 3c). The sensitivity analyses (Supplementary Information 4) demonstrate that the model is particularly sensitive to small biases, and probably more sensitive than measurements on paired materials. The CSRA dates are clearly compatible with the attribution of these pottery vessels to the Grossgartach ceramic phase based on their decorative motifs, and with the other radiocarbon dates for this group.

We then explored the introduction of a new food product—that is, milk—into Neolithic Europe by undertaking radiocarbon dating of animal fat residues, including dairy fats, that were recovered from early farming settlements with Linearbandkeramik (LBK) pottery (Fig. 1). These communities settled in central Europe from the early fifty-fourth century BC¹³. Animal fats in 12 potsherds from the earliest LBK contexts at 6 sites, in Poland, France, Germany and the Netherlands, produced radiocarbon dates that were modelled and shown to be compatible with the currency of LBK ceramics in northern and western Europe^{12,13} (Extended Data Figs. 3, 4 and Supplementary Information 5). Sensitivity analyses (Extended Data Fig. 4 and Supplementary Information 5) demonstrate that this model is more sensitive to older biases as we focused on early settlements, illustrating the direct dating of a new food commodity. The radiocarbon dates on the earliest dairy residues suggest that the practice began in 5385–5225 cal. BC (95% probability; start LBK lipid; Extended Data Fig. 3) and probably arrived with the earliest farmers in these areas. Thus, the linking of fatty acid structures with compound-specific carbon isotope values and CSRA dates provides a powerful means of directly dating prehistoric foodways and their introduction.

We next investigated pottery from the Sahara Desert to provide a test of the methodology for a region in which depositional conditions are very different from the temperate climes of northern Europe. The Takarkori rock shelter, located in the now hyper-arid area of the Acacus Mountains, southwest Libya, demonstrates evidence of animal exploitation based on rock art and archaeological finds¹⁴ (Extended Data Figs. 5, 6). Previous work revealed abundant adipose and dairy fat residues in fragments of the pottery vessels²⁸. Stratigraphy and radiocarbon dating of a range of materials (bone collagen, charred plant remains, dung, skin and enamel bioapatite) placed deposits associated with Middle Pastoral pottery in the sixth–fifth millennium cal. BC^{14,28,29}. The fatty acids from 5 potsherds, containing dairy fat (Extended Data Fig. 6b), produced uncalibrated radiocarbon ages of $5,993 \pm 28$ BP (TAK443), $5,979 \pm 28$ BP (TAK120), $5,493 \pm 28$ BP (TAK420), $5,348 \pm 24$ BP (TAK21) and $5,085 \pm 24$ BP (TAK1572). The CSRA dates were proven to be entirely compatible with the currency of Middle Pastoral Neolithic ceramics (Extended Data Fig. 6d and Supplementary Information 6), and the direct radiocarbon dating of dairy residues confirms that dairy in North Africa began as early as the end of the sixth millennium cal. BC^{14,28,29}. Although the model sensitivity is weak based on the small number of reference dates that it includes (Extended Data Fig. 7 and Supplementary Information 6), it demonstrates the possibility of dating potsherds from extremely arid burial conditions. In addition, direct dating of pottery lipids represents

Article

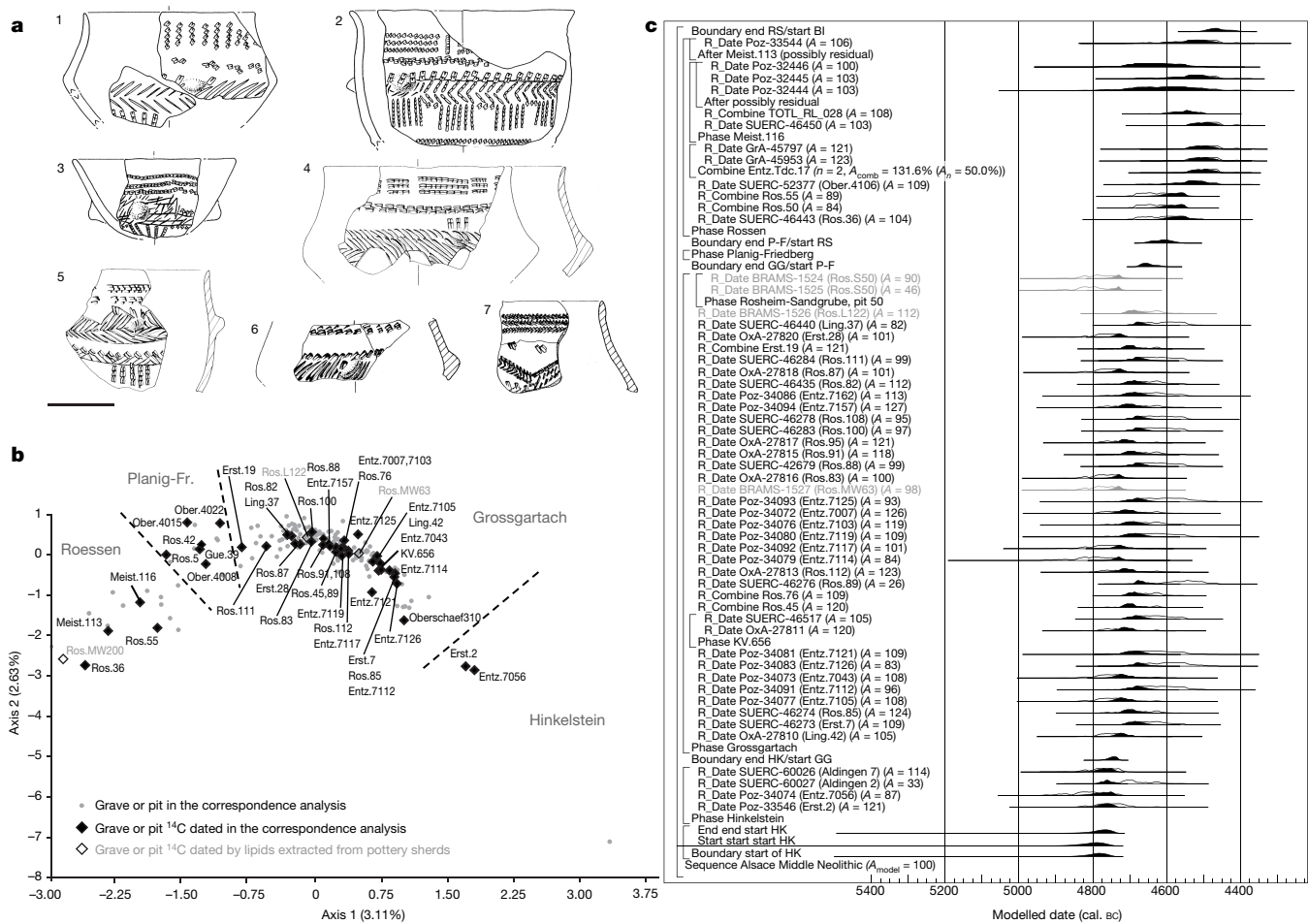


Fig. 3 | Drawings, correspondence analysis and radiocarbon dates of Neolithic vessels from Alsace (France) modelled using Bayesian statistics. **a**, Drawings of decorated pottery vessels from the Grossgartach group from pits 122 (1, 2), 50 (4, 5) and 63 (3, 6, 7) from which the undecorated potsherds dated in the model were recovered. Scale bar, 5 cm. **b**, Revised correspondence

analysis on the cultural assemblages (axis 1) and horizontal decorative motifs (axis 2), including features that contained the dated sherds from the Alsatian Neolithic groups. **c**, Revised statistical model of the Middle Neolithic with radiocarbon dates on pot lipids included in grey. The data are shown as described in Fig. 2c. A_{model} is the model agreement index.

a major contribution to ascertain the correct cultural attribution of materials found in loose sediments (organic sands), which are typical of desert environments and frequently found in highly disturbed sequences¹⁴.

Finally, archaeological excavations of several pits by the Museum of London Archaeology in advance of building works at Principal Place, London (PPL11) revealed one of the largest assemblages of Neolithic pottery recovered so far from the City of London or its immediate environs. Notably, the only finds other than pottery recovered from this deposit (lithics, bones and charred plant remains) were compromised by later disturbance and truncation. The assemblage comprised Neolithic plain and decorated bowls, consisting of thin-walled medium-sized open/neutral bowls, together with several smaller open bowls/cups (J.C. et al., manuscript in preparation). Similar material has been found elsewhere in the Thames Valley and beyond. Lipid-residue analyses revealed high concentrations of degraded animal fats in several sherds, which were shown by compound-specific $\delta^{13}\text{C}$ values to derive from dairy and adipose fats (Fig. 1c). Radiocarbon measurements of fatty acids from four plain sherds yielded uncalibrated ages of $4,911 \pm 27$ BP (PPL012), $4,742 \pm 22$ BP (PPL015), $4,652 \pm 26$ BP (PPL020) and $4,733 \pm 22$ BP (PPL021). A statistical model confirms that the pottery dates fit well within the currency of Plain Bowls in southern Britain¹⁵ (Extended Data Fig. 8 and Supplementary Information 7). The sensitivity analyses (Extended Data Fig. 9 and Supplementary Information 7)

are weaker in this case, but demonstrates the value of dating absorbed lipid residues in situations in which no other datable material exists. Our ability to undertake accurate radiocarbon dating of compound-specific fatty acids from pottery was invaluable in affording a temporal insight into some of the earliest traces of human activity in what is now the City of London.

In summary, the radiocarbon determinations of lipid residues from Neolithic pottery vessels presented above, modelled against site chronologies, establish the CSRA of fatty acids as a robust tool for archaeological dating. Importantly, our method and findings bring pottery vessels within the range of other archaeological materials that are routinely dated by radiocarbon. The importance of this advance to the archaeological community cannot be overstated. Pottery typology is the most widely used dating technique in the discipline, and thus the opportunity to anchor different kinds of pottery securely to the calendrical timescale will be of utmost practical importance. Notably, pottery often survives in circumstances in which other organic materials often do not and, therefore, archaeological questions relating to chronology that are currently intractable will come within the scope of our technologies.

Online content

Any methods, additional references, Nature Research reporting summaries, source data, extended data, supplementary information,

acknowledgements, peer review information; details of author contributions and competing interests; and statements of data and code availability are available at <https://doi.org/10.1038/s41586-020-2178-z>.

1. Orton, C. & Hughes, M. *Pottery in Archaeology* 2nd edn (Cambridge Univ. Press, 2014).
2. Evin, J., Gabasio, M. & Lefevre, J. C. Preparation techniques for radiocarbon dating of potsherds. *Radiocarbon* **31**, 276–283 (1989).
3. Hedges, R. M., Tierney, C. & Housley, R. A. Results and methods in the radiocarbon dating of pottery. *Radiocarbon* **34**, 906–915 (1992).
4. Gabasio, M., Evin, J., Arnal, G. B. & Andrieux, P. Origins of carbon in potsherds. *Radiocarbon* **28**, 711–718 (1986).
5. Casanova, E., Knowles, T. D. J., Williams, C., Crump, M. P. & Evershed, R. P. Use of a 700 MHz NMR microcryoprobe for the identification and quantification of exogenous carbon in compounds purified by preparative capillary gas chromatography for radiocarbon determinations. *Anal. Chem.* **89**, 7090–7098 (2017).
6. Casanova, E., Knowles, T. D. J., Williams, C., Crump, M. P. & Evershed, R. P. Practical considerations in high-precision compound-specific radiocarbon analyses: eliminating the effects of solvent and sample cross-contamination on accuracy and precision. *Anal. Chem.* **90**, 11025–11032 (2018).
7. Evershed, R. P. et al. Chemistry of archaeological animal fats. *Acc. Chem. Res.* **35**, 660–668 (2002).
8. Roffet-Salque, M. et al. From the inside out: upscaling organic residue analyses of archaeological ceramics. *J. Archaeol. Sci. Rep.* **16**, 627–640 (2017).
9. Coles, J. M. & Orme, B. J. Ten excavations along the Sweet Track (3200 bc). *Somerset Lev. Pap.* **10**, 5–45 (1984).
10. Hillam, J. et al. Dendrochronology of the English Neolithic. *Antiquity* **64**, 210–220 (1990).
11. Marciniaik, A. et al. Fragmenting times: interpreting a Bayesian chronology for the late Neolithic occupation of Çatalhöyük East, Turkey. *Antiquity* **89**, 154–176 (2015).
12. Denaire, A. et al. The cultural project: formal chronological modelling of the early and middle Neolithic sequence in Lower Alsace. *J. Archaeol. Method Theory* **24**, 1072–1149 (2017).
13. Jakucs, J. et al. Between the Vinča and Linearbandkeramik worlds: the diversity of practices and identities in the 54th–53rd centuries cal bc in Southwest Hungary and beyond. *J. World Prehist.* **29**, 267–336 (2016).
14. Biagiotti, S. & di Lernia, S. Holocene deposits of Saharan rock shelters: the case of Takarkori and other sites from the Tadrart Acacus Mountains (southwest Libya). *Afr. Archaeol. Rev.* **30**, 305–338 (2013).
15. Whittle, A. W. R., Healy, F. M. A. & Bayliss, A. *Gathering Time: Dating the Early Neolithic Enclosures of Southern Britain and Ireland* (Oxbow Books, 2011).
16. Wheeler, R. E. M. *Archaeology from the Earth* (Penguin, 1956).
17. Taylor, R. E. *Radiocarbon Dating, An Archaeological Perspective* (Academic, 1987).
18. Bronk Ramsey, C. Bayesian analysis of radiocarbon dates. *Radiocarbon* **51**, 337–360 (2009).
19. Barnett, W. & Hoopes, J. W. *The Emergence of Pottery: Technology and Innovation in Ancient Societies* (Smithsonian Institution Press, 1995).
20. Kuzmin, Y. The origins of pottery in East Asia: updated analysis (the 2015 state-of-the-art). *Doc. Praehist.* **42**, 1–11 (2015).
21. Stott, A. W. et al. Radiocarbon dating of single compounds isolated from pottery cooking vessel residues. *Radiocarbon* **43**, 191–197 (2001).
22. Evershed, R. P. Biomolecular archaeology and lipids. *World Archaeol.* **25**, 74–93 (1993).
23. Berstan, R. et al. Direct dating of pottery from its organic residues: new precision using compound-specific carbon isotopes. *Antiquity* **82**, 702–713 (2008).
24. Eglington, T. I., Aluwihare, L. I., Bauer, J. E., Druffel, E. R. M. & McNichol, A. P. Gas chromatographic isolation of individual compounds from complex matrices for radiocarbon dating. *Anal. Chem.* **68**, 904–912 (1996).
25. Coles, B. J. & Coles, J. M. *Sweet Track to Glastonbury: The Somerset Levels in Prehistory* 163–169 (Oxbow, 1986).
26. Reimer, P. J. et al. IntCal13 and Marine13 radiocarbon age calibration curves 0–50,000 years cal bp. *Radiocarbon* **55**, 1869–1887 (2013).
27. Roffet-Salque, M. et al. Evidence for the impact of the 8.2-kyBP climate event on Near Eastern early farmers. *Proc. Natl. Acad. Sci. USA* **115**, 8705–8709 (2018).
28. Dunne, J. et al. First dairying in green Saharan Africa in the fifth millennium bc. *Nature* **486**, 390–394 (2012).
29. Cherkinsky, A. & di Lernia, S. Bayesian approach to ^{14}C dates for estimation of long-term archaeological sequences in arid environments: the Holocene site of Takarkori Rockshelter, Southwest Libya. *Radiocarbon* **55**, 771–782 (2013).

Publisher's note Springer Nature remains neutral with regard to jurisdictional claims in published maps and institutional affiliations.

© The Author(s), under exclusive licence to Springer Nature Limited 2020

Article

Methods

Lipid extraction and isolation

Potsherds were selected on the basis of the presence of terrestrial animal fats (dairy and ruminant carcass fats) in the lipid residue to avoid any possible reservoir effect caused by the processing of aquatic products in pots. A piece of 1–10 g of the potsherd was sampled, according to the lipid concentration. The sherds were extracted in a glass culture tube using H_2SO_4 /MeOH (4% v/v, 3 × 8 ml, 70 °C, 1 h). The supernatants were centrifuged (2,500 rpm, 10 min) and combined into new culture tubes containing double-distilled water (5 ml). The lipids were extracted with *n*-hexane (4 × 5 ml), transferred into 3.5-ml vials and blown to dryness at room temperature under a gentle nitrogen stream. Subsequently, around 180 µl of *n*-hexane was added to obtain a concentration of fatty acid methyl esters (FAMEs) at 5 µg of C µl⁻¹ before transfer to an autosampler vial for isolation by pcGC.

The pcGC consisted of a Hewlett Packard 5890 series II gas chromatograph coupled to a Gerstel Preparative Fraction Collector by a heated transfer line. The pcGC was equipped with a column with a 100% poly(dimethylsiloxane) stationary phase (Rxi-1ms, 30 m × 0.53 mm inner diameter, 1.5 µm film thickness, Restek). Helium was used as the carrier gas at a constant pressure of 10 psi. The GC temperature programme started with an isothermal hold at 50 °C for 2 min, the temperature was increased to 200 °C at 40 °C min⁻¹, to 270 °C at 10 °C min⁻¹ and finally increased to 300 °C at 20 °C min⁻¹ and held for 8.75 min. The C_{16:0} and C_{18:0} FAMEs were injected (1 µl per run), separated and trapped 40 times per trapping sequence. Of the GC column effluent, 1% flows to the flame ionization detector, while the remaining 99% passes through a transfer line into the fraction collector, both of which were heated to 300 °C. Compounds were isolated based on their retention times⁶. The stationary phase degradation of the pcGC column and other sources of exogenous carbonaceous contamination were monitored on a Brucker Avance III HD 700 MHz NMR instrument following a previously published procedure^{5,6}.

Radiocarbon determinations and statistical analysis

The pcGC isolated compounds were transferred into Al capsules, after which they were combusted and graphitized in a Vario Microcube Elemental Analyser linked to an Automated Graphitisation System (AGE 3, IonPlus). All of the radiocarbon measurements were performed by the Bristol Accelerator Mass Spectrometer (BRAMS) facility at the University of Bristol. Data reduction was performed using the software BATS³⁰ (v.4.07). Radiocarbon dates obtained for FAMEs were corrected for the presence of added methyl carbon using a mass balance approach^{5,6,21} and reported as the conventional radiocarbon ages³¹ (Supplementary Information 1).

Two contemporaneous compounds (C_{16:0} and C_{18:0} fatty acids) were dated and every pair of statistically indistinguishable measurements (at the 95% significance level)³² was combined as a weighted average before Bayesian chronological modelling using OxCal v.4.2 and v.4.3^{18,33} and the currently internationally agreed radiocarbon calibration curve for the Northern Hemisphere, IntCal13²⁶. The compatibility of the radiocarbon dates on absorbed fatty residues with existing sites and regional chronologies was assessed by including the lipid radiocarbon dates into existing statistical frameworks in a position defined by archaeological information (for example, stratigraphy or seriation). Their compatibility with the existing chronologies were achieved by: (1) comparison of posterior density estimates for key modelled parameters with equivalent date estimates or known age by dendrochronology; (2) using the individual and model agreement indices^{18,33} in models containing fatty acid dates; and (3) comparing posterior density estimates for key parameters from models that include the fatty acid dates to a model that does not include the fatty acid dates (Supplementary

Information 1). The sensitivity of existing chronological models to the addition of the new radiocarbon measurements was evaluated as above, after deliberately biasing the radiocarbon dates on pottery vessels to varying degrees while assessing the effect on posterior density estimates for the key parameters and indices of agreements (Supplementary Information 1–7).

Reporting summary

Further information on research design is available in the Nature Research Reporting Summary linked to this paper.

Data availability

All data generated during this study are included in the Article, Extended Data Figs. 1–9, Extended Data Table 1 and Supplementary Information.

Code availability

The codes used in OxCal for statistical modelling are provided in the Supplementary Information.

30. Wacker, L., Christl, M. & Synal, H.-A. BATS: a new tool for AMS data reduction. *Nucl. Instrum. Methods Phys. Res. B* **268**, 976–979 (2010).
31. Stuiver, M. & Polach, H. A. Discussion reporting of ¹⁴C data. *Radiocarbon* **19**, 355–363 (1977).
32. Ward, G. K. & Wilson, S. R. Procedures for comparing and combining radiocarbon age determinations: a critique. *Archaeometry* **20**, 19–31 (1978).
33. Bronk Ramsey, C. Radiocarbon calibration and analysis of stratigraphy: the OxCal program. *Radiocarbon* **37**, 425–430 (1995).
34. Stuiver, M. & Reimer, P. J. Extended ¹⁴C data base and revised CALIB 3.0 ¹⁴C age calibration program. *Radiocarbon* **35**, 215–230 (1993).

Acknowledgements We thank the European Research Council for funding an advanced grant (NeoMilk, FP7-IDEAS-ERC/324202) and a proof-of-concept grant (LipDat, H2020 ERC-2018-PoC/812917) to R.P.E., financing a PhD to E. Casanova and postdoctoral contract to M.R.-S. and J.S., and a postdoctoral contract to E. Casanova; the BRAMS facility for the radiocarbon measurements, establishment of which was jointly funded by the NERC, BBSRC and University of Bristol; P. Monaghan for his help with the radiocarbon sample preparation; the Polish National Science Centre (decision DEC-2012/06/M/H3/00286) for financing the work in the upper levels at Çatalhöyük; the Department of Antiquities in Tripoli, Libya for permits and Sapienza University of Rome and Italian Ministry of Foreign Affairs for funding the fieldwork in Libya; MOLA (Museum of London Archaeology) for excavating and providing potsherds from Principal Place (PPL1), London EC2/E1; and B. Schnitzler from the Palais Rohan for accessing the material from Rosheim, A. Mulot from the Achéologie Alsace (Centre of Conservation and Study) for accessing the material from Ensisheim, R. W. Schmitz from the LVR-Landes Museum Bonn for accessing the material from Königshoven 14 and R. Brunning from the South West Heritage Trust for sharing excavation photographs of the Sweet Track.

Author contributions R.P.E. conceived the project. E. Casanova, R.P.E. and A. Bayliss wrote the paper. E. Casanova, T.D.J.K. and R.P.E. developed the method for dating lipids. E. Casanova, J.D. and T.G. performed the preparation of pottery vessels for radiocarbon analysis. E. Casanova and T.D.J.K. generated the radiocarbon measurements and performed data analysis. A. Bayliss undertook the statistical modelling of the radiocarbon dates. M.Z.B. advised on the stratigraphic sequence of the TP area of Çatalhöyük East. A.M. performed the stratigraphic analysis of the TP area of Çatalhöyük East and chronological analysis of the LBK from the Polish lowlands and M.K. helped with the selection and provided the pottery vessels from these sites. C.J. and P.L. excavated the Alsatian sites. A. Denaire and P.L. performed the correspondence analysis of the Alsace region. S.d.L. advised on the stratigraphic sequence and pottery analysis of Takarkori and R.R. studied the pottery assemblage. E. Casanova, M.R.-S. and J.S. sampled the LBK sites. M.R.-S. coordinated and processed the analyses of sherds from the LBK culture and from Çatalhöyük East. A. Barclay advised on project design. B.C. directed excavations of the Sweet Track and S.M. provided the pottery vessels. E. Claßen analysed the material and advised sampling for Königshoven 14. M.I. excavated and provided vessels from Cuiry-lès-Chaudardes. I.v.W. excavated and advised sampling from The Netherlands and P.v.d.V. analysed the material. A. Daykin excavated the site of Principal Place, London EC2/E1 as project manager and J.C. studied the pottery material.

Competing interests The authors declare no competing interests.

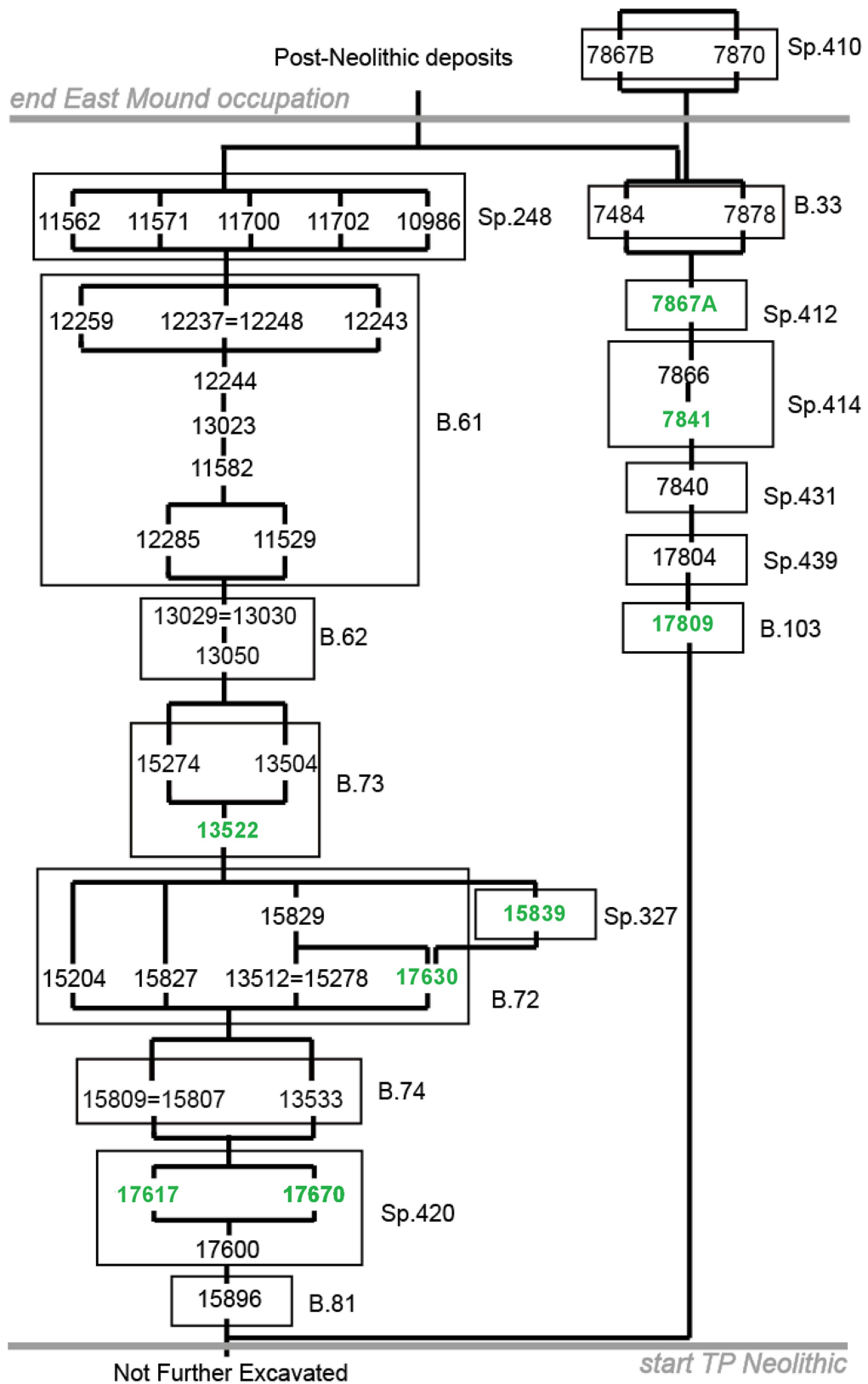
Additional information

Supplementary information is available for this paper at <https://doi.org/10.1038/s41586-020-2178-z>.

Correspondence and requests for materials should be addressed to R.P.E.

Peer review information *Nature* thanks Graeme Barker and the other, anonymous, reviewer(s) for their contribution to the peer review of this work.

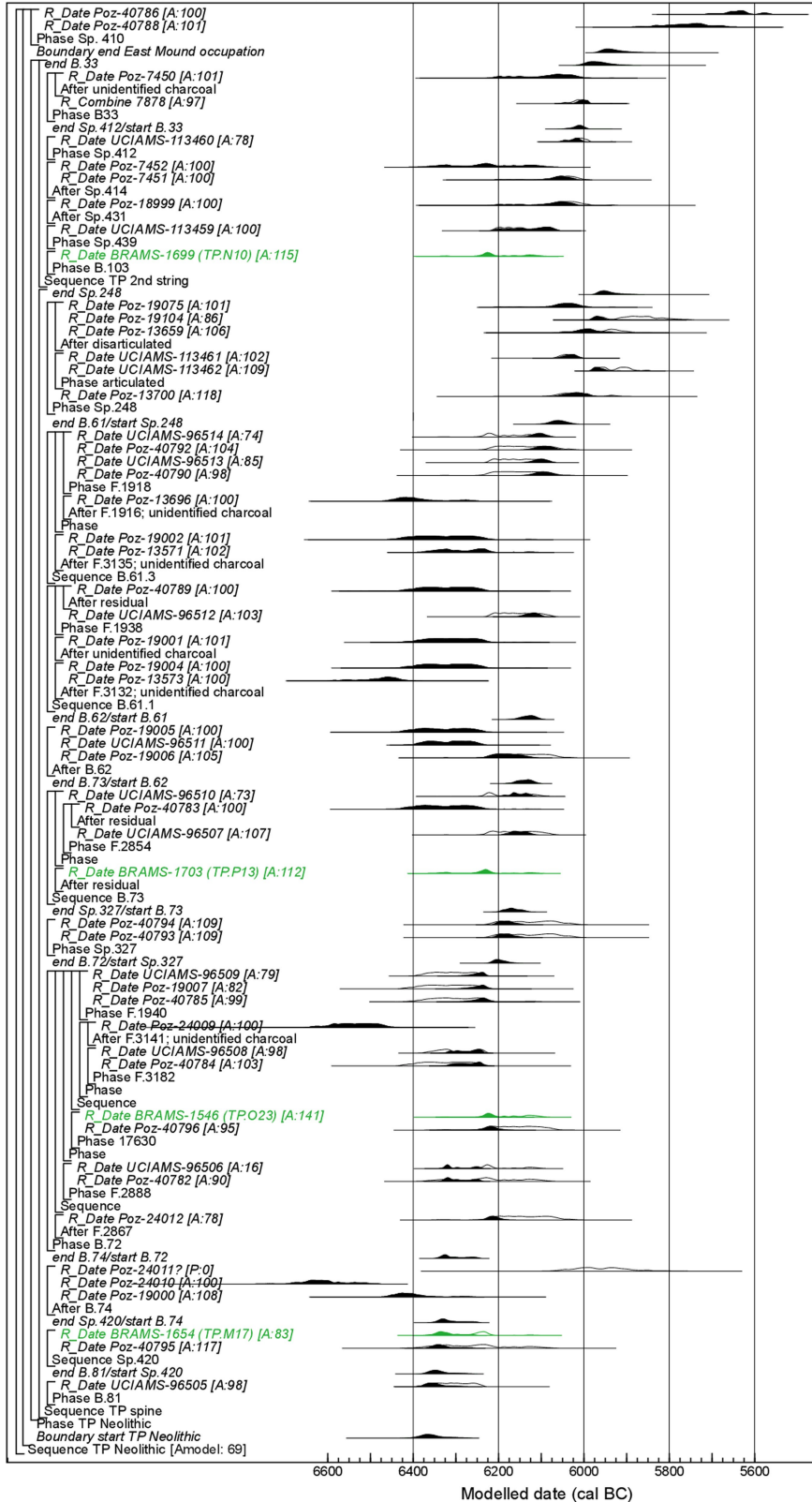
Reprints and permissions information is available at <http://www.nature.com/reprints>.



Extended Data Fig. 1 | Schematic showing the stratigraphic information of the Neolithic occupation of the TP area at Çatalhöyük (Turkey). This information was included in the chronological model defined in Extended Data Fig. 2. Contexts containing potsherds dated in this study are highlighted in green.

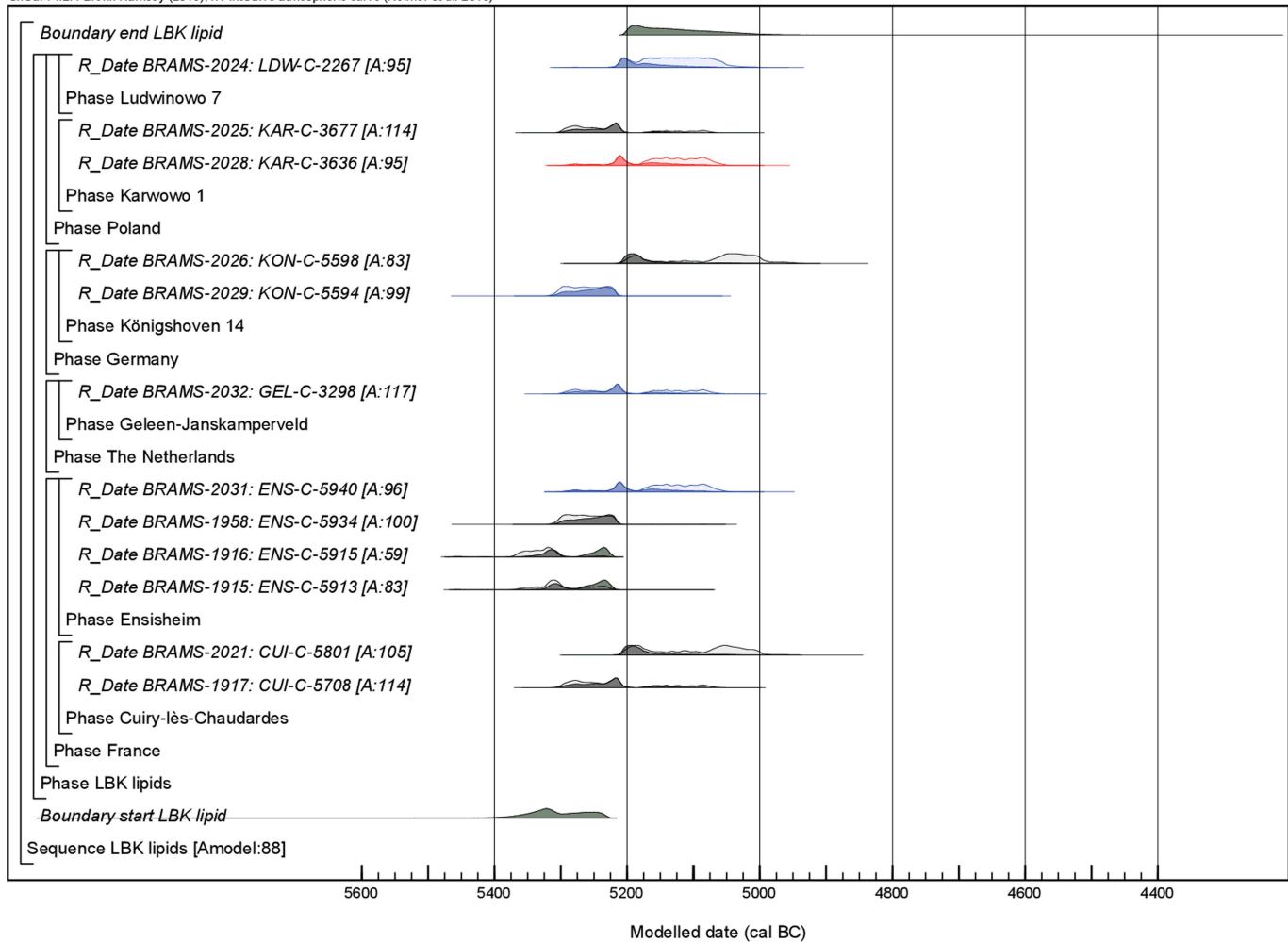
Article

OxCal v4.2.4 Bronk Ramsey (2013); r:1 IntCal13 atmospheric curve (Reimer *et al.* 2013)



Extended Data Fig. 2 | Probability distributions of dates from Neolithic deposits in the TP area at Çatalhöyük, Turkey. Data include the results on absorbed fatty acids in pottery sherds listed in Extended Data Table 1. Each distribution represents the relative probability that an event occurs at a particular time. For each date, two distributions are plotted: one in outline, which is the result of a simple radiocarbon calibration, and a solid one, based on the chronological model used. The distributions in green correspond to the potsherds, distributions in black show the pre-existing chronology.

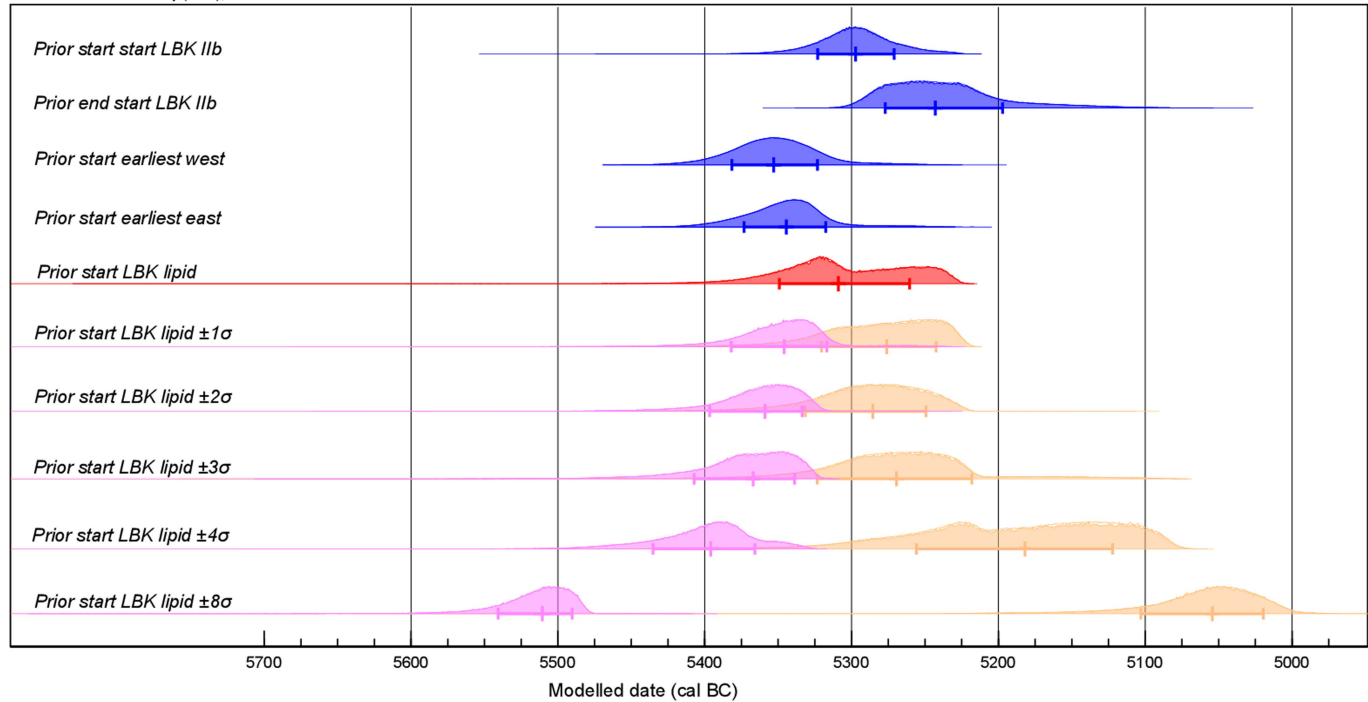
Distributions other than those relating to particular samples correspond to aspects of the model. For example, the distribution 'end East Mound occupation' is the estimated date at which the Neolithic occupation of the East Mound ended at Çatalhöyük. Measurements followed by a question mark and shown in outline have been excluded from the model for reasons described in table 1 of a previous study³¹ and are simple calibrated dates³⁴. The large square brackets down the left side, along with the OxCal keywords, define the overall model exactly.



Extended Data Fig. 3 | Probability distributions of radiocarbon dates from absorbed fatty acids in LBK ceramics. Data on absorbed fatty acids are listed in Extended Data Table 1. Black, dairy; blue, ruminant adipose; red, non-ruminant adipose. Data are shown as described for Extended Data Fig. 2.

Article

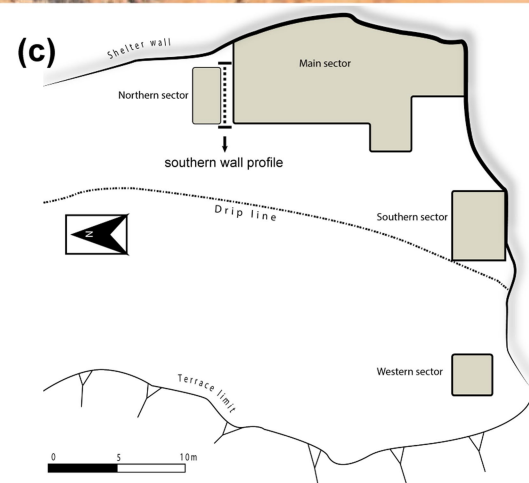
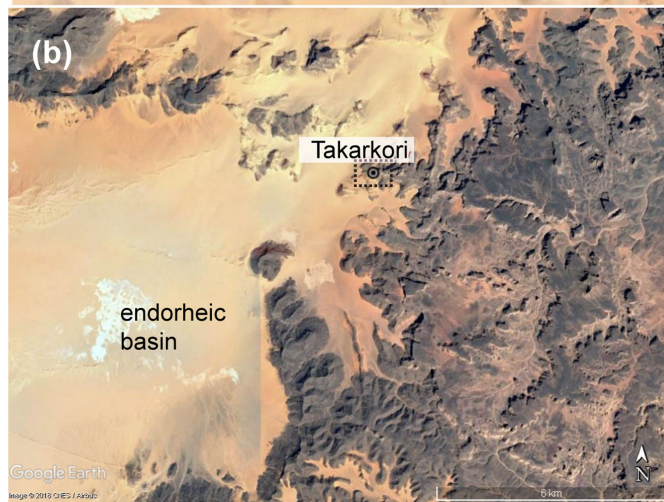
OxCAL v4.3.2 Bronk Ramsey (2017); r:5



Extended Data Fig. 4 | Sensitivity analyses of radiocarbon dates on LBK ceramics.

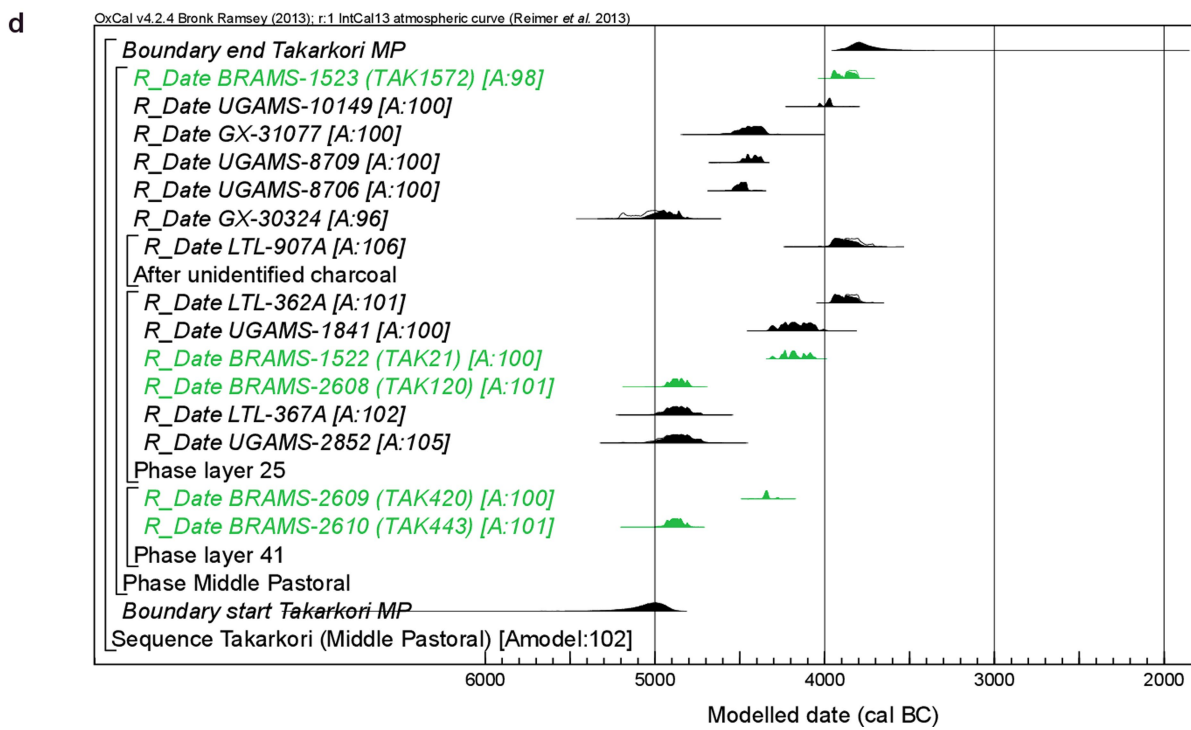
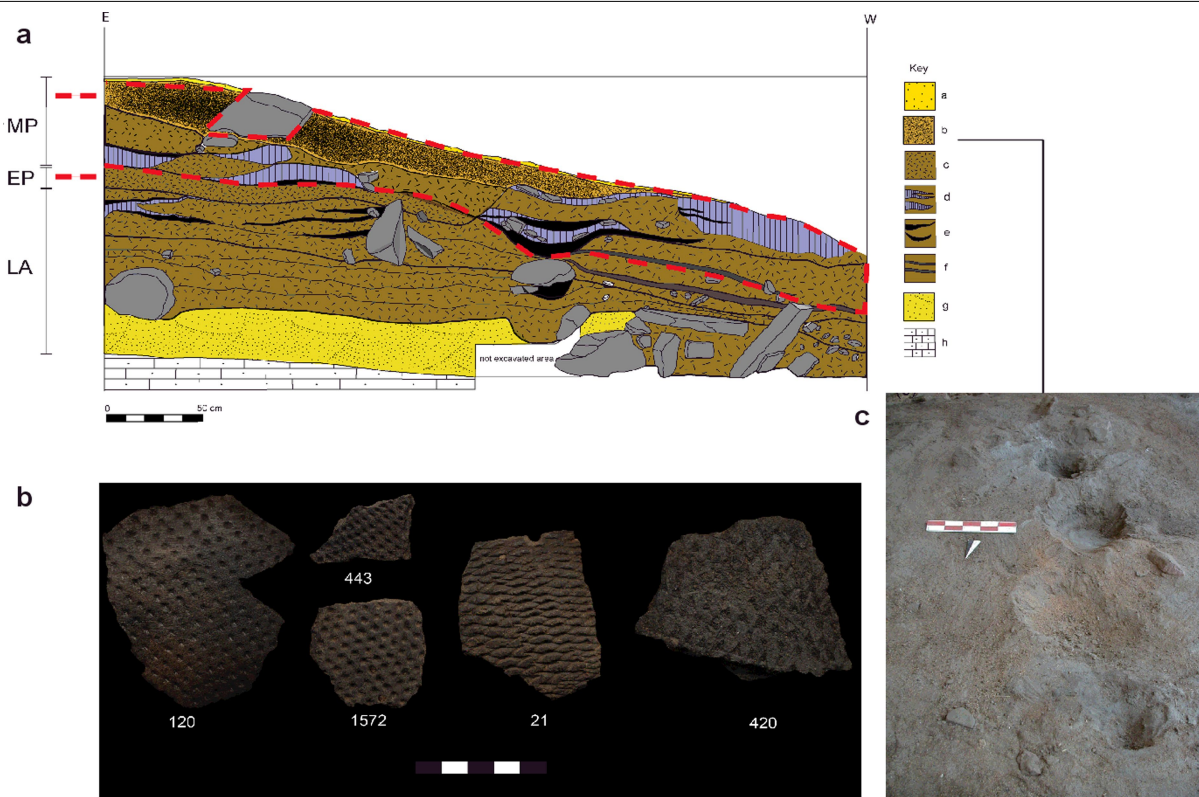
Key parameters for the start of the use of LBK ceramics (blue distribution)—derived from the models defined in Extended Data Fig. 3, figure 8 of a previous study¹², and figures 18, 19 (model 1), 20, 21 (model 2) and 22, 23 (model 3) of a previous publication¹³—were compared with the start of LBK

lipids presented in Extended Data Fig. 3 (red distributions), and subsequently deliberately biased by 1σ , 2σ , 3σ , 4σ and 8σ to younger (orange distributions) and older (pink distributions) values. Some distributions may have been truncated.



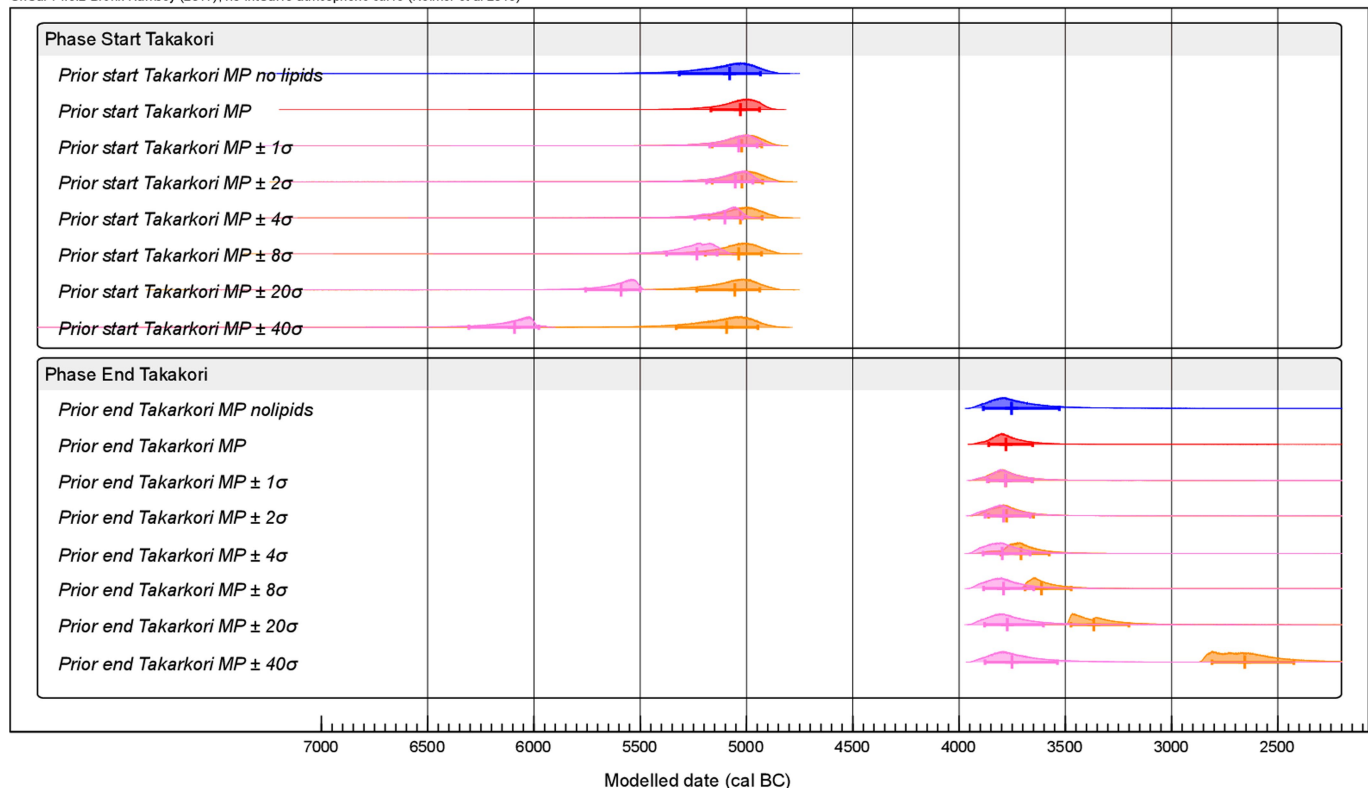
Extended Data Fig. 5 | The Tadrart Acacus Mountains in southwest Libya. a, b, The Wadi Takarkori area (dashed rectangle). **c,** Schematic plan of the excavated areas. All sampled sherds come from the main sector.

Article



Extended Data Fig. 6 | Site stratigraphy, photographs of potsherds and radiocarbon dates of Middle Pastoral pottery vessels from Takarkori (Libya) modelled using Bayesian statistics. **a**, Stratigraphic context of sampled potsherds from Takarkori east–west profile of the southern wall of the Takarkori north–south (Extended Data Fig. 5). (a) aeolian sand; (b) sand rich in organic matter; (c) lenses of undecomposed plant remains; (d) ash; (e) charcoal; (f) slurry deposit; (g) eroded sand from the wall; (h) bedrock. **b**, Photographs of

the five potsherds analysed showing typical Middle Pastoral decorative patterns. **c**, Example of temporally and spatially wide deposit of organic sands (detail of layer 25, Takarkori main sector). **d**, Statistical model of the Middle Pastoral period showing the comparison of pot lipid dates (in green) with previous radiocarbon measurements. Data are shown as described for Extended Data Fig. 2.

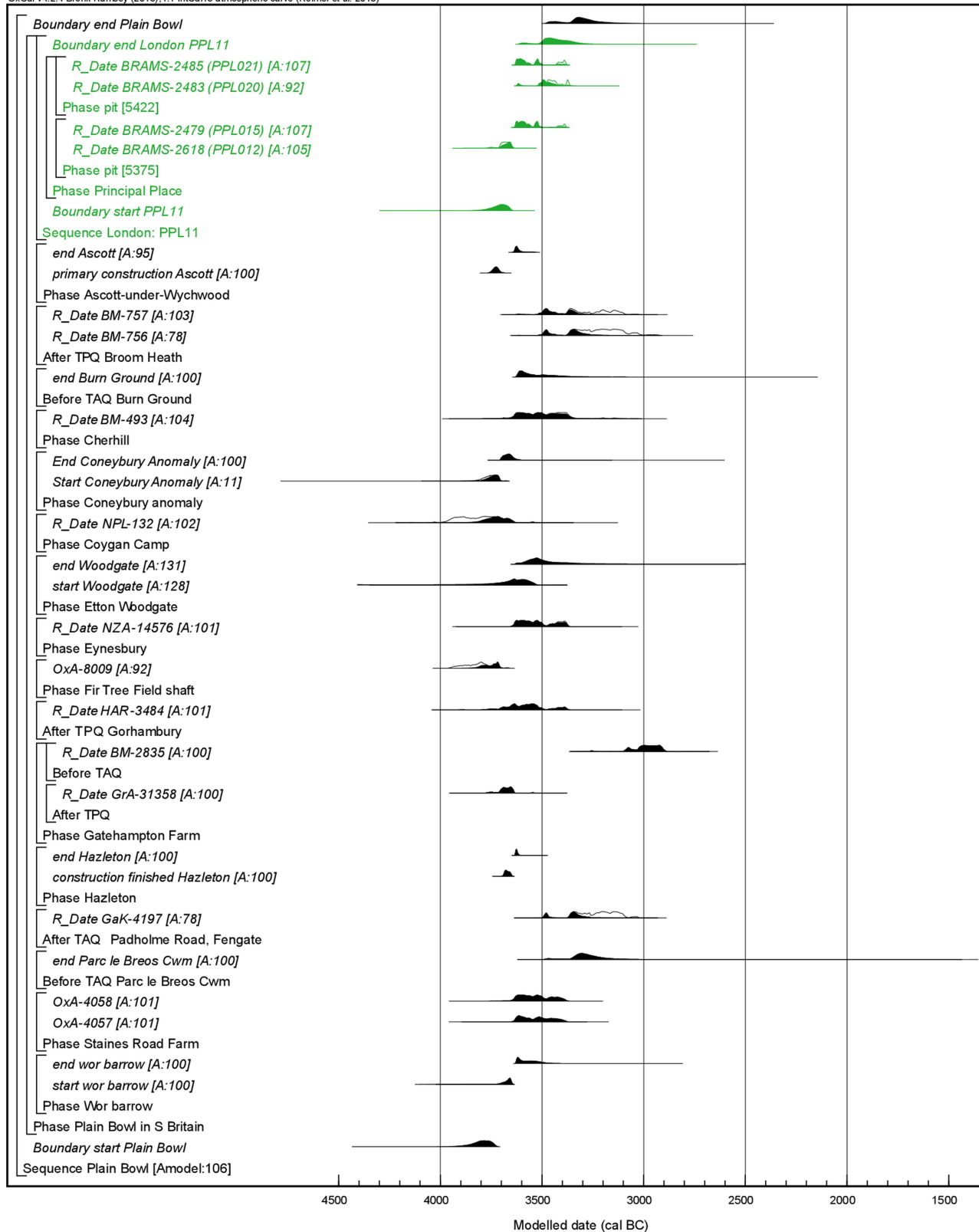


Extended Data Fig. 7 | Sensitivity analyses of radiocarbon dates on vessels from Takarkori rock shelter, Libya. Probability distributions for the beginning and end Middle Pastoral period ceramics from Takarkori rock shelter, Libya (no pot lipid dates) compared with those of the model shown in

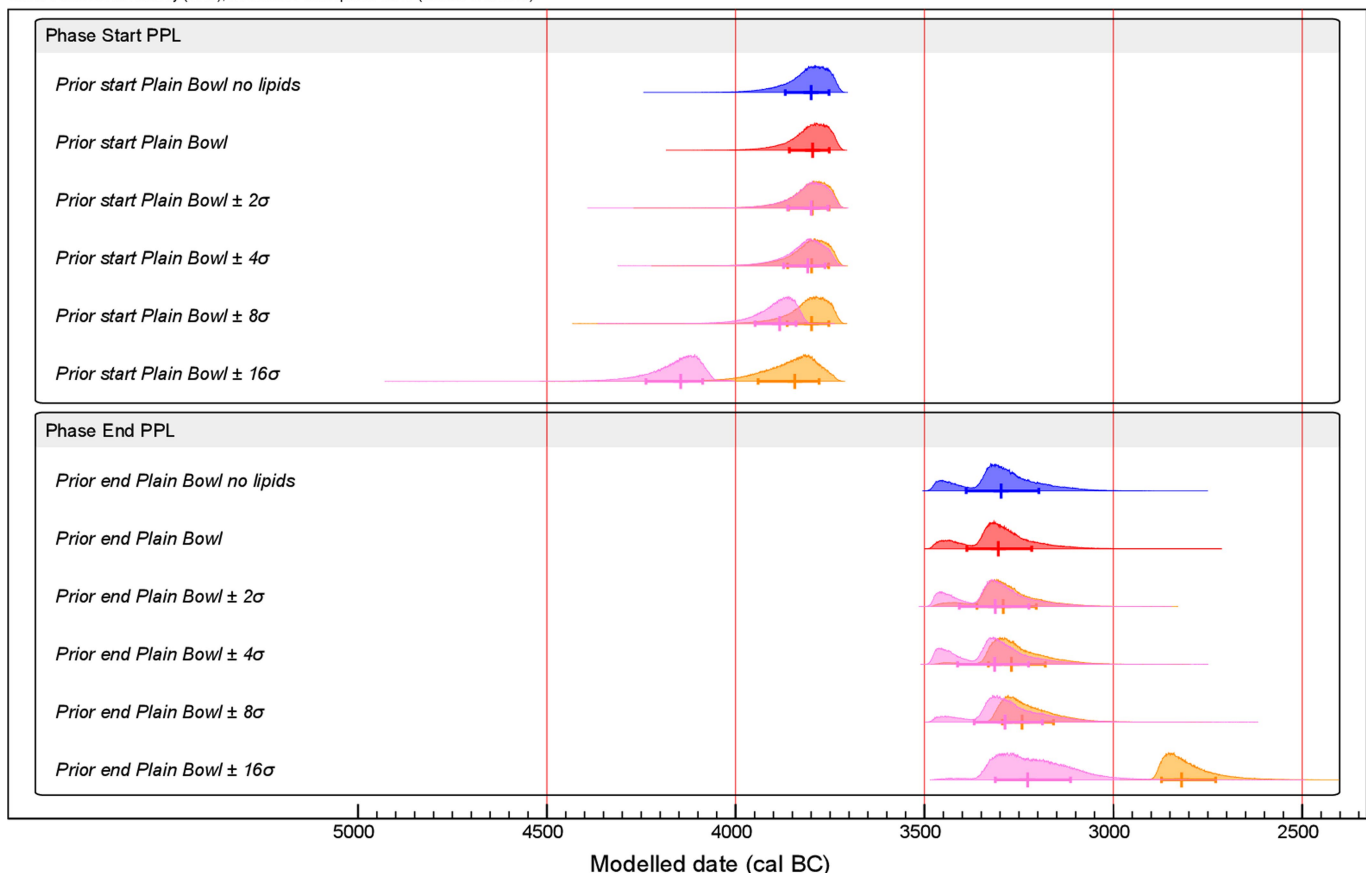
the Extended Data Fig. 6d and models including fatty acid dates that were deliberately biased by 1σ , 2σ , 4σ , 8σ , 20σ and 40σ . Data are shown as described for Extended Data Fig. 4.

Article

OxCAL v4.2.4 Bronk Ramsey (2013); r:1 IntCal13 atmospheric curve (Reimer et al. 2013)



Extended Data Fig. 8 | Probability distributions of dates associated with the use of early Neolithic Plain Bowl pottery in southern Britain. Prior distributions have been taken from the models described in the text and in the Supplementary Information. Data are shown as described for Extended Data Fig. 2.



Extended Data Fig. 9 | Sensitivity analyses of radiocarbon dates on vessels from Principal Place, London. Probability distributions of the start and end of early Neolithic Plain Bowl pottery in southern Britain compared with those of

the model shown in Extended Data Fig. 8 and models including fatty acid dates that were deliberately biased by 2σ , 4σ , 8σ and 16σ . Data are shown as described for Extended Data Fig. 4.

Article

Extended Data Table 1 | Summary of radiocarbon dates of lipids preserved in pottery vessels

Site	Location	Potsherd #	Description	C ⁶ (µg/g)	Laboratory#	C _{16:0} age	C _{18:0} age	Combined age	Reference
Sweet Track	Somerset levels, England	SW1	Carinated Bowl, refitted sherd	13,806	BRAMS-1520	5,105 ± 33	5,114 ± 32	5,110 ± 25	9, 10, 25
		SW2	Carinated Bowl, refitted sherd	4,900	BRAMS-1521	5,089 ± 38	5,094 ± 32	5,092 ± 26	
Çatalhöyük East 'TP Area'	Konya, Turkey	TP.M17	Holemouth jar, single sherd	393	BRAMS-1654	7,338 ± 42	7,416 ± 39	7,382 ± 31	11, 27
		TP.N10	Holemouth jar, refitted sherd	575	BRAMS-1699	7,318 ± 29	7,378 ± 30	7,348 ± 25	
		TP.O23	Holemouth jar, refitted sherd	1,390	BRAMS-1546	7,290 ± 36	7,375 ± 32	7,340 ± 27	
		TP.P13	Holemouth jar, single sherd	362	BRAMS-1703	7,328 ± 36	7,394 ± 29	7,364 ± 25	
Rosheim 'Sandgrube'	Lower Alsace, France	ROS-C-4596	Coarse Kumpf, single sherd	973	BRAMS-1526	5,810 ± 30	5,798 ± 30	5,804 ± 25	12
		ROS-C-4600	Coarse Kumpf, refitted sherd	4,163	BRAMS-1527	5,897 ± 36	5,909 ± 35	5,904 ± 28	
		ROS-C-4644	Fine Kumpf, single sherd	6,064	BRAMS-1525	5,937 ± 33	5,926 ± 30	5,931 ± 26	
		ROS-C-4657	Coarse Kumpf, single sherd	1,914	BRAMS-1524	5,885 ± 37	5,934 ± 34	5,912 ± 28	
Ensisheim 'Ratfeld'	Upper Alsace, France	ENS-C-5913	Coarse Kumpf, single sherd	1,177	BRAMS-1915	6,345 ± 31	6,303 ± 31	6,324 ± 26	12, 13
		ENS-C-5915	Coarse Kumpf, single sherd	771	BRAMS-1916	6,383 ± 32	6,314 ± 33	6,348 ± 26	
		ENS-C-5934	Coarse Kumpf, single sherd	1,645	BRAMS-1958	6,282 ± 30	6,258 ± 30	6,270 ± 25	
		ENS-C-5940	Coarse Kumpf, single sherd	2,082	BRAMS-2031	6,162 ± 33	6,239 ± 30	6,206 ± 26	
Cuiry-lès- Chaudardes	Aisne, France	CUI-C-5708	Coarse Kumpf, single sherd	881	BRAMS-1917	6,252 ± 34	6,218 ± 36	6,236 ± 27	12, 13
		CUI-C-5801	Coarse Kumpf, single sherd	9,886	BRAMS-2021	6,138 ± 30	6,134 ± 30	6,136 ± 25	
Königshoven 14	Rhineland, Germany	KON-C-5594	Coarse Kumpf, single sherd	531	BRAMS-2029	6,253 ± 29	6,298 ± 29	6,276 ± 24	12, 13
		KON-C-5598	Coarse Kumpf, single sherd	1,023	BRAMS-2026	6,106 ± 34	6,139 ± 34	6,123 ± 27	
Geleen- Janskamperveld	Graetheide, The Netherlands	GEL-C-3298	Coarse Kumpf, single sherd	577	BRAMS-2032	6,188 ± 31	6,253 ± 29	6,224 ± 25	12, 13
Karwowo 1	Pomerania, Poland	KAR-C-3636	Coarse Kumpf, single sherd	3,316	BRAMS-2028	6,176 ± 30	6,230 ± 30	6,204 ± 25	12, 13
		KAR-C-3677	Coarse Kumpf, single sherd	1,900	BRAMS-2025	6,255 ± 30	6,214 ± 32	6,236 ± 26	
Ludwinowo 7	Kuyavia, Poland	LDW-C-2267	Coarse Kumpf, single sherd	323	BRAMS-2024	6,173 ± 36	6,179 ± 30	6,177 ± 26	12, 13
Takarkori Rockshelter	Acacus mountains, Libya	TAK 21	Decorated, single sherd	9,503	BRAMS-1522	5,362 ± 33	5,331 ± 32	5,348 ± 24	14, 28, 29
		TAK1572	Decorated, single sherd	3,558	BRAMS-1523	5,099 ± 38	5,071 ± 32	5,085 ± 24	
		TAK 120	Decorated, single sherd	5,593	BRAMS-2608	6,008 ± 35	5,949 ± 35	5,979 ± 28	
		TAK 420	Decorated, single sherd	1,119	BRAMS-2609	5,487 ± 34	5,498 ± 35	5,493 ± 28	
		TAK 443	Decorated, single sherd	17,217	BRAMS-2610	6,021 ± 35	5,962 ± 35	5,992 ± 28	
Principal Place	London, England	PPL012 (<1814>)	Plain Bowl, single sherd	713	BRAMS-2618	4,894 ± 34	4,928 ± 33	4,911 ± 27	15
		PPL015 (<1845>)	Plain Bowl, refitted sherd	1,999	BRAMS-2479	4,708 ± 33	4,771 ± 30	4,742 ± 22	
		PPL020 (<1850>)	Plain Bowl, refitted sherd	3,660	BRAMS-2483	4,628 ± 40	4,670 ± 34	4,652 ± 26	
		PPL021 (<1819>)	Plain cup, single sherd	2,985	BRAMS-2485	4,732 ± 32	4,734 ± 30	4,733 ± 22	

Vessel descriptions, lipid concentrations and conventional radiocarbon ages (as defined previously³¹ and calculated according to previously published methods³⁰) of C_{16:0} and C_{18:0} fatty acids (which passed the internal quality control) extracted from pottery vessels.

Corresponding author(s): Richard P. Evershed

Last updated by author(s): Jan 22, 2020

Reporting Summary

Nature Research wishes to improve the reproducibility of the work that we publish. This form provides structure for consistency and transparency in reporting. For further information on Nature Research policies, see [Authors & Referees](#) and the [Editorial Policy Checklist](#).

Statistics

For all statistical analyses, confirm that the following items are present in the figure legend, table legend, main text, or Methods section.

n/a Confirmed

- The exact sample size (n) for each experimental group/condition, given as a discrete number and unit of measurement
- A statement on whether measurements were taken from distinct samples or whether the same sample was measured repeatedly
- The statistical test(s) used AND whether they are one- or two-sided
Only common tests should be described solely by name; describe more complex techniques in the Methods section.
- A description of all covariates tested
- A description of any assumptions or corrections, such as tests of normality and adjustment for multiple comparisons
- A full description of the statistical parameters including central tendency (e.g. means) or other basic estimates (e.g. regression coefficient) AND variation (e.g. standard deviation) or associated estimates of uncertainty (e.g. confidence intervals)
- For null hypothesis testing, the test statistic (e.g. F , t , r) with confidence intervals, effect sizes, degrees of freedom and P value noted
Give P values as exact values whenever suitable.
- For Bayesian analysis, information on the choice of priors and Markov chain Monte Carlo settings
- For hierarchical and complex designs, identification of the appropriate level for tests and full reporting of outcomes
- Estimates of effect sizes (e.g. Cohen's d , Pearson's r), indicating how they were calculated

Our web collection on [statistics for biologists](#) contains articles on many of the points above.

Software and code

Policy information about [availability of computer code](#)

Data collection

Data (radiocarbon dates) were acquired on a MICADAS AMS system using BATS software (v4.07)

Data analysis

The software BATS (v4.07) was used for data reduction analysis of radiocarbon dates and OxCal (v4.2 and v4.3) for chronological modeling

For manuscripts utilizing custom algorithms or software that are central to the research but not yet described in published literature, software must be made available to editors/reviewers. We strongly encourage code deposition in a community repository (e.g. GitHub). See the Nature Research [guidelines for submitting code & software](#) for further information.

Data

Policy information about [availability of data](#)

All manuscripts must include a [data availability statement](#). This statement should provide the following information, where applicable:

- Accession codes, unique identifiers, or web links for publicly available datasets
- A list of figures that have associated raw data
- A description of any restrictions on data availability

All data generated during this study are included in the main article, extended data and supplementary information.

Field-specific reporting

Please select the one below that is the best fit for your research. If you are not sure, read the appropriate sections before making your selection.

Life sciences

Behavioural & social sciences

Ecological, evolutionary & environmental sciences

For a reference copy of the document with all sections, see nature.com/documents/nr-reporting-summary-flat.pdf

Life sciences study design

All studies must disclose on these points even when the disclosure is negative.

Sample size	The vessels dated were selected based on their lipid concentration which determined the number of samples radiocarbon dated in this paper
Data exclusions	Radiocarbon dates that did not pass the internal criterion (chi-square test on C16 and C18 fatty acids radiocarbon ages) explained in the SI document were excluded from chronological modeling
Replication	No replication of radiocarbon dates was undertaken due to the destructive nature of the radiocarbon dating technique, and limited sample availability. Tests of repeatability have been presented in a previously published paper Casanova et al. (2018) cited in this paper.
Randomization	Randomization was not relevant to the study. Our aim was to check the accuracy of radiocarbon dates determined for pottery vessels from secure and well defined archaeological contexts.
Blinding	Blinding was not relevant to the study, see as above.

Reporting for specific materials, systems and methods

We require information from authors about some types of materials, experimental systems and methods used in many studies. Here, indicate whether each material, system or method listed is relevant to your study. If you are not sure if a list item applies to your research, read the appropriate section before selecting a response.

Materials & experimental systems		Methods	
n/a	Involved in the study	n/a	Involved in the study
<input checked="" type="checkbox"/>	<input type="checkbox"/> Antibodies	<input checked="" type="checkbox"/>	<input type="checkbox"/> ChIP-seq
<input checked="" type="checkbox"/>	<input type="checkbox"/> Eukaryotic cell lines	<input checked="" type="checkbox"/>	<input type="checkbox"/> Flow cytometry
<input checked="" type="checkbox"/>	<input type="checkbox"/> Palaeontology	<input checked="" type="checkbox"/>	<input type="checkbox"/> MRI-based neuroimaging
<input checked="" type="checkbox"/>	<input type="checkbox"/> Animals and other organisms		
<input checked="" type="checkbox"/>	<input type="checkbox"/> Human research participants		
<input checked="" type="checkbox"/>	<input type="checkbox"/> Clinical data		